

Experimental dynamic identification of backlash using skeleton methods

Tegoeh Tjahjowidodo*, Farid Al-Bender, Hendrik Van Brussel

Mechanical Engineering Department, Division PMA, Katholieke Universiteit Leuven, Celestijnenlaan 300B, B3001 Heverlee, Belgium

Received 9 June 2005; received in revised form 27 October 2005; accepted 4 November 2005

Available online 15 December 2005

Abstract

In this paper, we present a practical application of non-linear system identification, namely to a mechanical system with a backlash component, based on the skeleton curve reconstruction technique. In the case presented, the identification procedure employs the instantaneous amplitude and frequency of the input and the output of the base motion system under certain forced excitation.

Hilbert transform analysis is a well-known method to extract these instantaneous characteristics; however, it is strictly exact only if the signal is weakly damped. A time–frequency representation technique, the Wavelet transform analysis, is therefore introduced to overcome this problem. The instantaneous characteristics in the signals can be obtained from the ridges and skeletons of the Wavelet transform. We apply both methods to the case study and compare the results, showing that the Wavelet-based extraction is generally more accurate than the Hilbert-analysis-based method. We show further that it is possible to obtain good non-linear identification results using either of the methods.

© 2005 Elsevier Ltd. All rights reserved.

Keywords: Backlash; Ridge; Skeleton; Hilbert transform; Wavelet analysis

1. Introduction

Almost all physical engineering systems exhibit non-linear behaviour to some degree in practice. Generally, the causes of non-linearities in structural systems can be classified into four sources. They may arise from the effect of material properties, geometric structure, force boundary conditions and displacement boundary conditions [1]. Material non-linearities commonly give rise to very complex phenomena, since the properties depend not only on current variable state but also on the past history of the state. A common example of this is the hysteresis with non-local memory such as found in the friction in presliding/prerolling regime [2,3]. The second type of non-linearity, the geometric non-linearity, manifests itself as a change in the modal parameters of a structure, namely the restoring and damping forces, with changes in the structure deformations during motion. This type of non-linearity conceptually is simpler than the former one, in the sense that the response does not depend on the history of the input even though it may be amplitude, velocity and frequency

*Corresponding author. Tel.: +32 16 322515; fax: +32 16 322987.

E-mail address: tgoeh.tjahjowidodo@mech.kuleuven.ac.be (T. Tjahjowidodo).

dependent. The last two types of non-linearity sources, which concern the dependence of the applied force and displacement on the deformation of the structure, are of relatively less occurrence and interest than the former two. This paper is primarily concerned with the second class of non-linearity source, namely the geometric one, in particular, an extreme case thereof, namely backlash.

Since classical linear methods applied to non-linear structures provide no means of describing the arising complex phenomena, the distinction between linear and non-linear systems is becoming a crucial problem. Two levels of interest may be distinguished; namely (i) detection of non-linearities and (ii) characterisation/identification (modal model, parameter quantification, ...) of non-linearities. In regard to the first point, many different procedures have been developed to detect the presence of the non-linearities in a system as summarised in Ref. [4]. The most popular method is by using the coherence function or by inspecting the Frequency Response Function (FRF) distortion in the Nyquist plot. The latter technique can be improved by applying the Hilbert transformation [5], based on the fact that the Hilbert transform (HT) of the FRF of a linear structure reproduces the original FRF, and any departure from this can be attributed to non-linear effects. As regards the second point, methods of characterizing the type of non-linearity itself are being developed in more detail.

For system identification, the free vibration analysis, which is popular for linear systems, is however not so suitable for non-linear system identification where the natural frequencies are amplitude dependent. The function relating the natural frequencies to the amplitude, namely the so-called skeleton curve, of a non-linear system shows a deviation from the horizontal straight line of the linear system case. Every typical non-linearity of a modal parameter in the system, e.g. the restoring and damping force, has a unique form of skeleton curve. The analysis of the topography of the skeleton curve for different non-linear modal parameters is summarised in Ref. [6]. Further analysis of the obtained skeleton curve can provide us with the estimated characteristics of the restoring and damping forces after some mathematical manipulations are applied.

Feldman [7] has proposed the method of FreeVib, which observes free vibration response of a system after shock excitation, to identify the geometrical non-linear modal parameters of the system using the HT. Extensive studies on the effectiveness of extracting the instantaneous amplitude and frequency can be found in [8,9], while the practical application of this technique for the purpose of damage diagnosis of rotors was presented by Feldman and Seibold [10].

However, for a great number of real engineering systems, in particular those with high damping, free vibration analysis is not suitable due to the fact that the transient response occurs in a very short time duration so that the observation sample is not adequate for FreeVib identification. In order to overcome this problem, Feldman proposed the ForceVib method [11]. In this method (see Section 2 below), the system under investigation is excited using a suitable excitation input and after some mathematical manipulation, the skeleton curve can be obtained as a function of the envelope and the instantaneous frequencies of the output response as well as the excitation input.

Although simple and effective, the aforementioned HT-based identification techniques are limited by some conditions. Extraction of the envelope signal and its instantaneous frequencies, which is necessary for the skeleton reconstruction purpose, using HT is strictly exact only if the real-value (original) signal is asymptotic, where the signal has slowly varying amplitudes compared with the phase variations. In particular, Ruzzene et al. [12] demonstrated that this technique gives higher error levels the higher the damping present in the system. Furthermore, even if the signals analysed are asymptotic, the HT method still requires a signal filtration step.

The Wavelet transform technique has gained popularity in the area of time–frequency representation (TFR) study and system identification field. This technique is actually developed as an alternative approach to the STFT to overcome the resolution problem in the latter transformation technique. Staszewski [13] extensively demonstrated the application for identification of geometrical non-linearity in the mechanical structures. He extracted the instantaneous properties of the transient response using the ridges of its Wavelet transform and reconstructed the skeleton curve to identify the modal parameters in the system. He also extended his analysis to the identification of a two-degree-of-freedom system. In a subsequent paper, Staszewski and Chance [14] verified the corresponding theoretical study on a real experimental set-up. They implemented the identification technique on a test rig comprising a mass suspended on a non-linear spring. The test set-up was designed and built in such a way as to minimise the damping in the system. Therefore, the transient response of the system after shock excitation can be observed sufficiently.

However, there are hardly any instances in the literature of the application of those types of system identification to systems comprising high damping. This is one of the aims of this paper. The general aim is to develop an effective identification technique for (geometrically) non-linear mechanical systems by observing a forced response and the excitation input of the system. In particular, this paper also presents the practical application to a real mechanical system with a backlash component, which is considered as a base motion system. The technique developed in this paper is based on instantaneous properties extraction of the output and input of the system via the Wavelet transform analysis. At the end, the paper compares and contrasts the extraction results using Wavelet and HT analysis in case of skeleton identification showing their possibilities and limitations. Obviously, those methods are applicable when the response is not chaotic. The case of a chaotic response to which non-linear systems are often liable is treated in [15].

In the following, Section 2 describes the theoretical basis of the methods. Section 3 describes the experimental set-up and formulates a detailed mechanical model of the system. Section 4 discusses the analysis, while the results will be presented and discussed in Section 5. Finally, appropriate conclusions are drawn in Section 6.

2. Theoretical basis

This section outlines the tools, which are necessary for further implementation of skeleton identification methods.

2.1. Forcevib method [7,11]

A large number of signals, including vibration of system with geometric non-linearities, can be converted to analytic signals in complex time and represented in the form of the combination of an envelope and an instantaneous phase [7]. Let us consider the following forced vibration equation of a single-degree-of-freedom system:

$$\ddot{y} + 2h_0(A)\dot{y} + \omega_0^2(A)y = f/m, \tag{1}$$

where y is the response signal, f is the forced excitation signal, m is the mass of the system, h_0 and ω_0 are the symmetrical viscous damping and stiffness characteristic of the system, respectively, which depend on the amplitude (A). According to the main properties of the non-overlapping spectra of HT, Feldman [11] shows that Eq. (1) can be converted by HT to the analytic signal form:

$$\dot{Y} + 2h_0(A)\dot{Y} + \omega_0^2(A)Y = F/m, \tag{2}$$

where $Y(t) = y(t) + j\tilde{y}(t) = A(t)e^{j\varphi(t)}$ is an analytic signal of the response of the system. Here, $\tilde{y}(t)$ is the HT of the real-value signal $y(t)$, while $F(t)$ is the analytic signal of the forced excitation.

Substituting the analytic signal forms of $Y(t)$ and $F(t)$ together with the two derivatives of $Y(t)$, i.e.

$$\begin{aligned} \dot{Y}(t) &= Y(t)[\dot{A}(t)/A(t) + j\omega(t)], \\ \ddot{Y}(t) &= Y(t)[\ddot{A}(t)/A(t) - \omega^2(t) + 2j\dot{A}(t)\omega(t)/A(t) + j\dot{\omega}(t)] \end{aligned}$$

into Eq. (2), one can derive the representation of the corresponding modal parameters:

$$Y \left[\frac{\ddot{A}}{A} - \omega^2 + \omega_0^2 + 2h_0 \frac{\dot{A}}{A} + j \left(2 \frac{\dot{A}}{A} \omega + \dot{\omega} + 2h_0 \omega \right) \right] = F/m. \tag{3}$$

Solving two equations for the real and imaginary parts from Eq. (3), one can write the expressions for instantaneous modal parameters as

$$\omega_0^2(t) = \omega^2 + \frac{\alpha(t)}{m} - \frac{\beta(t)\dot{A}}{A\omega m} - \frac{\ddot{A}}{A} + \frac{2\dot{A}^2}{A^2} + \frac{\dot{A}\dot{\omega}}{A\omega}, \tag{4}$$

$$h_0(t) = \frac{\beta(t)}{2\omega m} - \frac{\dot{A}}{A} - \frac{\dot{\omega}}{2\omega}, \tag{5}$$

where ω is the time derivative of the instantaneous phase ϕ , while α and β are the real and imaginary parts of input and output signals ratio $F(t)/Y(t) = \alpha(t) + j\beta(t)$, respectively.

2.2. Wavelet transform

Ruzzene et al. [12] showed that Hilbert-transform-based envelope and instantaneous frequency extraction introduces errors when the system is damped. In order to avoid this difficulty, in this paper, the Wavelet analysis is used as an alternative way in estimating the instantaneous properties.

Wavelet analysis is done in a similar way to the short-time Fourier transform (STFT), in the sense that the signal is multiplied with a function (the *mother wavelet*, similar to the window function in STFT), and the transform is computed separately for different segments of the time-domain signal.

The Wavelet transform of a real-valued signal $y(t)$ is defined as follows:

$$W(s, \tau) = \frac{1}{\sqrt{|s|}} \int_{-\infty}^{+\infty} y(t) \psi^* \left(\frac{t - \tau}{s} \right) dt. \quad (6)$$

As seen in Eq. (6), the transformed signal is a function of the *translation*, τ , which corresponds directly to time, *scale/dilation*, s , which relates to frequency information indirectly, and $\psi(t)$ as a *mother wavelet*. In this paper we use the popular function of Complex Morlet Wavelet [16]:

$$\psi(t) = \sqrt{\pi f_b} e^{j\omega_c t} e^{-t^2/f_b}, \quad (7)$$

where f_b is the bandwidth parameter and $\omega_c = 2\pi f_c$ is the centre frequency.

The term translation is used in the same sense as it is used in the STFT; it is related to the location of the window as that is shifted through the signal. Obviously, this term corresponds to time information in the transform domain. However, Wavelet Analysis does not have a frequency parameter. Instead, it has a scale parameter, which can be used to define the frequency information.

Analogous to Eq. (1), any response of a vibration system generally can be written as a function of its envelope and instantaneous phase as follows:

$$y(t) = A(t) \cos \varphi(t) \quad (8)$$

In the frequency domain, the spectrum of $y(t)$ at every instant of time, t_0 , is

$$Y(\omega) = \pi A(t_0) e^{j\theta} [\delta(\omega - \omega_n(t_0)) + \delta(\omega + \omega_n(t_0))], \quad (9)$$

where θ is the phase lag, $\omega_n(t_0)$ is the time derivative of $\varphi(t)$ in time t_0 and δ is the delta function.

Therefore, we have the modulus and phase of the Wavelet representation, which can be used for envelope and instantaneous frequency extraction [13]:

$$|W(s, \tau)| = \pi^2 f_b \sqrt{|s|} A(t) e^{-\frac{f_b}{4}(s\omega_n - \omega_c)^2}, \quad \angle W(s, \tau) = \omega\tau + \theta. \quad (10)$$

As an example, let us consider an impulse response of a viscously damped single-degree-of-freedom linear system. Mathematically, the impulse response can be written as

$$x(t) = A e^{-\zeta\omega_n t} \cos(\omega_d t + \phi_0).$$

where A is the magnitude, ω_n is the undamped frequency, ω_d is the damped frequency, ϕ_0 is the phase lag and ζ is the damping ratio.

The impulse response signal together with its envelope and instantaneous frequency estimation based on HT and Wavelet analysis can be seen in Fig. 1.

In the figure, we can see the extraction results of the envelope and instantaneous frequency signal. The extractions obtained based on Wavelet transform technique show less ripples compared to the ones from HT; however, the Wavelet has a drawback due to the *edge effect*. The windowing process by the *mother wavelet* when the transform is computed at the corresponding time instant causes errors of envelope extraction at the beginning and at the end of the signal. However, this limitation can be minimised by selecting a narrow bandwidth parameter of the mother Wavelet.

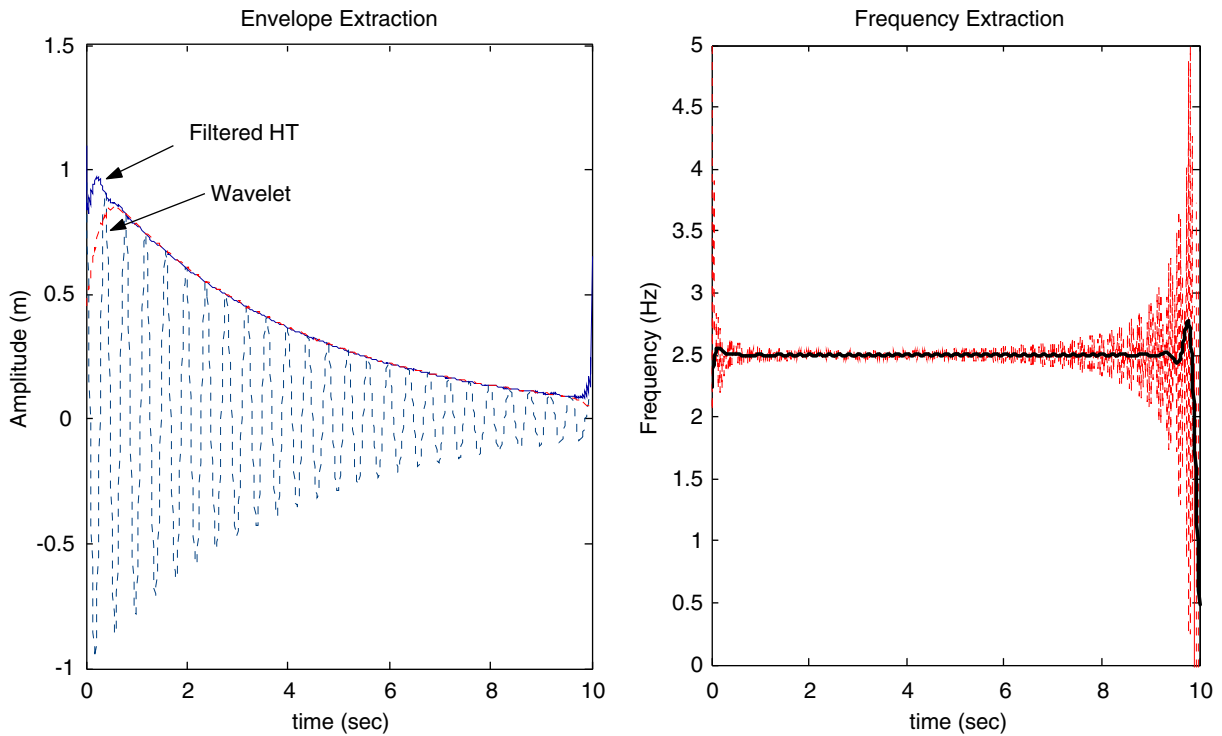


Fig. 1. Envelope and instantaneous frequency extraction of damped impulse response based on Hilbert and Wavelet transform: The left plot shows the damped signal together with the envelope extractions using Hilbert (after 0.05% filtration) and Wavelet analysis; dashed line: the original damped signal; solid lines: envelope extraction results. The instantaneous frequency extractions are shown in the right side for both techniques; dashed line: Hilbert-based frequency extraction; solid line: Wavelet-based frequency extraction.

The right panel of Fig. 1 shows the instantaneous frequency estimation of the impulse response system. It is clearly seen that the Wavelet analysis has improved the instantaneous frequency estimation. This technique succeeds in minimising the ripples that might occur in Hilbert technique without using any filtration procedures.

As a second example, we will consider a damped chirp signal with initial frequency of 0 Hz. The frequency of this signal continues to increase at a constant rate, until it reaches 10 Hz in 10 s. We can see in the left panel of Fig. 2 the corresponding damped chirp signal together with its envelope extraction based on both techniques. In this case we see more superiority in the Wavelet analysis, since the HT introduces much more ripples than that of the first example. However, the Wavelet analysis still suffers from the edge effect. The right figure shows the extraction of instantaneous frequency.

2.3. Base motion system

Commonly, most mechanical systems are characterised by force–displacement (or velocity); however, in some cases the system under investigation can be considered as a base motion system, where both input and output are displacements.

In the case of base motion system (Fig. 3), where the excitation input is taken in the form of displacement, we need a little mathematical manipulation to reformulate Eq. (1). The displacement equation form of this problem can be written as

$$\ddot{y} + 2h_0(A)\dot{y} + \omega_0^2(A)y = 2h_0(A)\dot{x} + \omega_0^2(A)x, \tag{11}$$

where x is the displacement input.

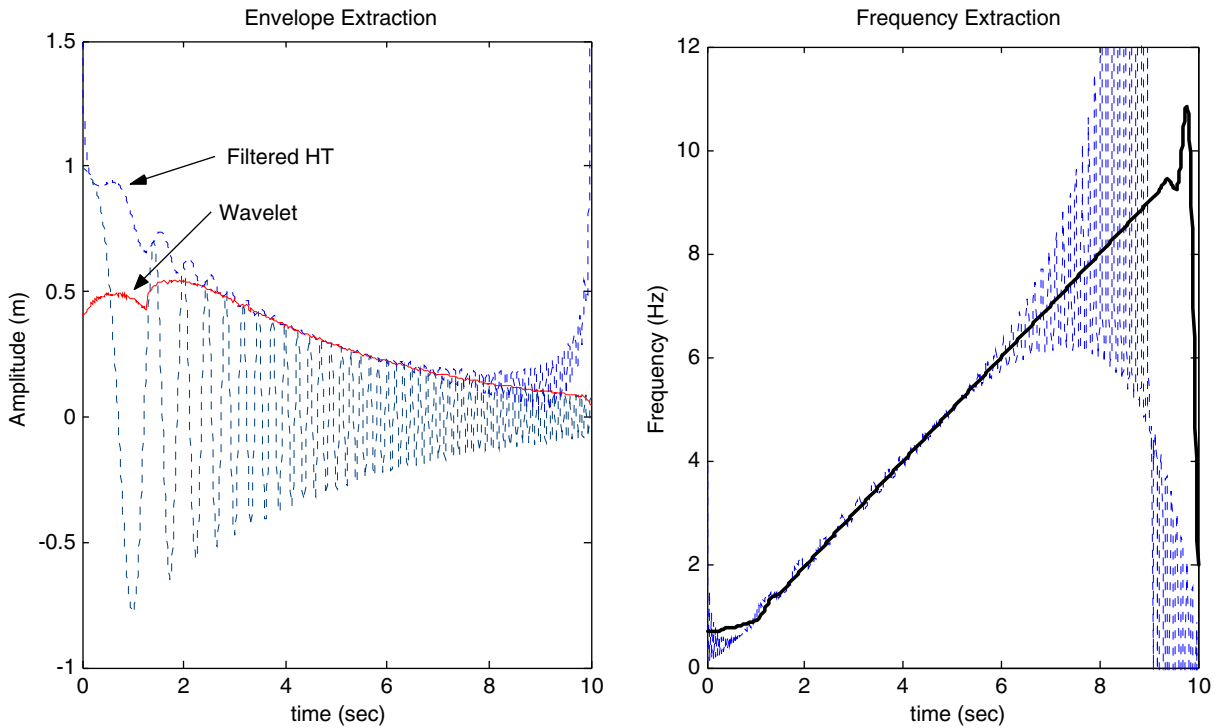


Fig. 2. Envelope and instantaneous frequency extraction of damped-chirp signal based on Hilbert and Wavelet transform: The left plot shows the damped-chirp signal together with the envelope extractions using Hilbert (after 0.05% filtration) and Wavelet analysis; dashed line: original chirp signal; solid lines: envelope extraction results. The instantaneous frequency extractions are shown in the right side for both techniques; dashed line: Hilbert-based frequency extraction; solid line: Wavelet-based frequency extraction.

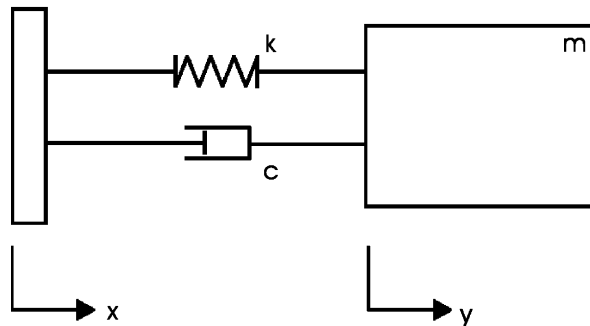


Fig. 3. Schematic of base motion system: mass m is excited by displacement input of x yielding output displacement of y . The two motion points x and y are connected using spring k and damper c .

If we introduce z as the relative motion between x and y ($z = x - y$), we may rewrite Eq. (11) as

$$\ddot{z} + 2h_0(A)\dot{z} + \omega_0^2(A)z = -\ddot{x}. \tag{12}$$

Taking $-\ddot{x}$ as input in Eq. (1), we can proceed to identify the modal parameters of the system as before.

3. Test set-up and experiment

An experimental investigation was carried out on the outer (second) link of a two-link mechanism as shown in Fig. 4. The aim of this experiment is to identify the backlash size of the second link joint. For this purpose,

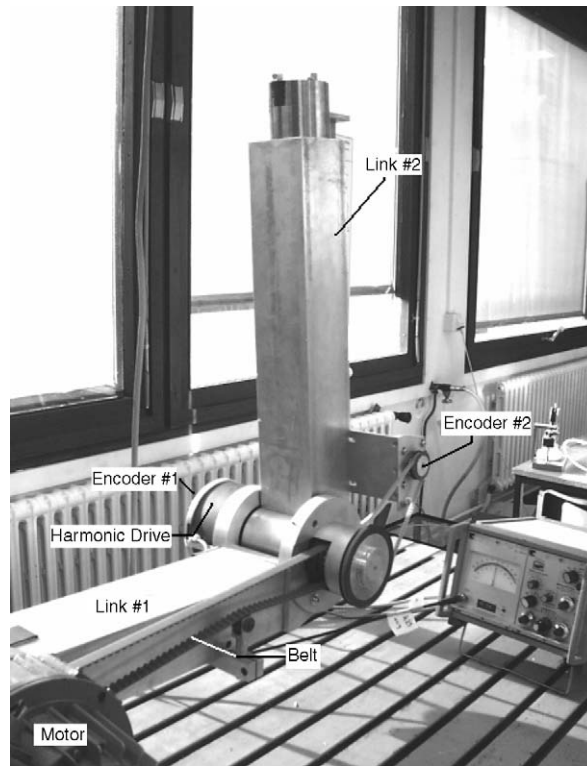


Fig. 4. Set-up of a two-link mechanism on site.

certain degree of backlash (approximately 1.5°) was introduced in the joint of this link. The first link was kept fixed while the second one was made to oscillate over a certain range. This link was driven by a servomotor through a geared belt and a harmonic drive. The harmonic drive is used as a strong reduction of the angular rotation of the motor.

The vibration responses were measured by two rotary encoders. The first encoder measured the angular motion input to the harmonic drive and the second one measured the relative oscillation between the first and second link. Therefore, the first encoder might be considered to measure the excitation input of a *base motion system* in displacement form, while the second encoder measured the response of that base motion system.

Fig. 5 depicts the schematic force balance of link#2 of the two-link system. The link is supported at its joint by a non-linear rotational spring and damper. The support of this link has a specified rotational motion, ϕ , which is the ‘displacement’ input, and is measured by the first encoder. The angular motion of link #2 is represented by θ .

The non-linear differential equation of motion of the system shown in Fig. 5 can be obtained easily as:

$$J\ddot{\theta} + c(A)\dot{\theta} + \{k(A) - mgL\}\theta = c(A)\dot{\phi} + k(A)\phi. \tag{13}$$

In the notation of Eq. (11), i.e. replacing y by θ and x by ϕ , we get

$$\ddot{y} + 2h_0(A)\dot{y} + \{\omega_0^2(A) - C\}y = 2h_0(A)\dot{x} + \omega_0^2(A)x, \tag{14}$$

where $C = mgL/J$ is an additional stiffness due to the link weight, m is the mass of the link, L is the coordinate of the centre of gravity of the link and J equals the link’s moment of inertia about its joint.

In the notation of Eq. (12), Eq. (14) becomes

$$\ddot{z} + 2h_0(A)\dot{z} + \omega_0^2(A)z = -\ddot{x} + Cy, (z = y - x). \tag{15}$$

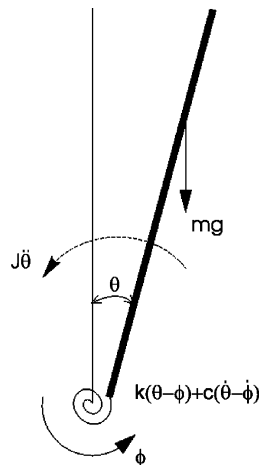


Fig. 5. Force balance diagram of link #2: Displacement input of ϕ degree oscillates link #2 having mass of m yielding displacement output of θ degree. The link is joined to the first link (kept fix) using a non-linear spring $k(\theta-\phi)$ and damping $c(\dot{\theta}-\dot{\phi})$.

If we refer to the transformation from displacement equation to the complex-analytic signal form from Ref. [7], by analogy we can transform Eq. (15) into a complex-analytic signal form:

$$\ddot{Z} + 2h_0(A)\dot{Z} + \omega_0^2(A)Z = -\ddot{X} + CY. \quad (16)$$

4. Signal analysis

The experiments were conducted by inputting a linear chirp signal to the motor. The initial frequency of this signal is 0 Hz. The frequency continues to increase at constant rate, reaching 12 Hz in 30 s. The oscillation response measured by encoder #1, which later will be considered as the displacement input of the second link, is given in Fig. 6, while the relative motion between the second and first link is given in Fig. 7, and the relative motion between responses measured by both encoders, z in Eq. (15), is shown in Fig. 8. In the figures, the dashed lines represent the size of the backlash. It is clearly seen in the latter figure that for a certain part of the time axis, the relative motion is larger than the backlash size in the joint. Beyond the time 16.25 s, which corresponds approximately to 6.5 Hz of instantaneous excitation frequency, the relative motion of the links falls far below the size of backlash. This occurs due to insufficient energy of excitation. Such a problem, which is difficult to avoid, might cause unsatisfactory skeleton curve reconstruction, which is essential in non-linear modal parameter identification.

In order to check the validity of these identification techniques, the system has been modally identified at the edge of backlash. Fig. 9 shows the FRF of the system obtained through shock excitation using impact hammer. The link was preloaded using a low stiffness spring to eliminate non-linearity due to the backlash; hence, the link was resting on one of the edges of the backlash.

The natural frequency of the system is approximately 11 Hz, while from the mass line we can estimate the moment of inertia of the link to be approximately equal to 3.16 kgm^2 (the estimation of moment of inertia based on its geometric calculation is 2.84 kgm^2). It is necessary to define the inertia of the system, since Eqs. (4) and (5) include modal mass value, which is unknown a priori.

4.1. Modification in non-linear modal parameters calculation

Some obvious modifications of non-linear modal parameter estimation procedures in Eq. (3) should be made in order to conform to the base motion case, since we are dealing with displacement input and displacement output in the system.

The displacement input $x(t)$ in complex-analytic form appearing in Eq. (16) can be written as: $X(t) = x(t) + j\hat{x}(t) = B(t) \exp[j\psi_x(t)]$.

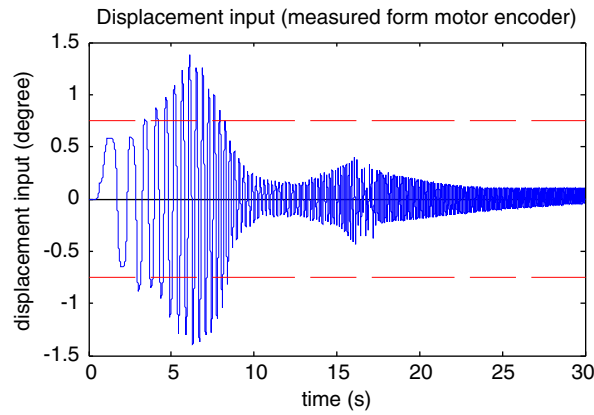


Fig. 6. Displacement input to the system measured by encoder #1: The solid line represents the input, while the dashed line shows the size of the backlash in the system.

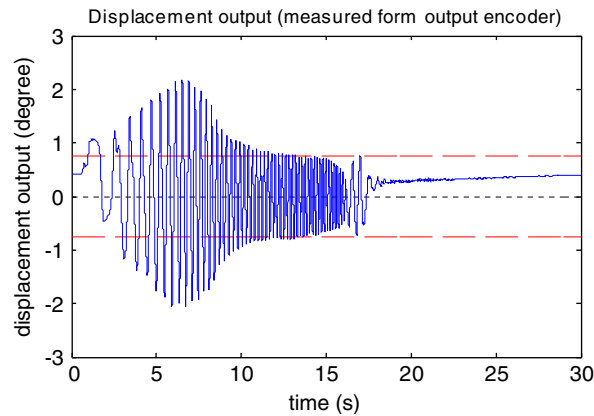


Fig. 7. Oscillation response measured by encoder #2: The solid line represents the response, while the dashed line shows the size of the backlash in the system.

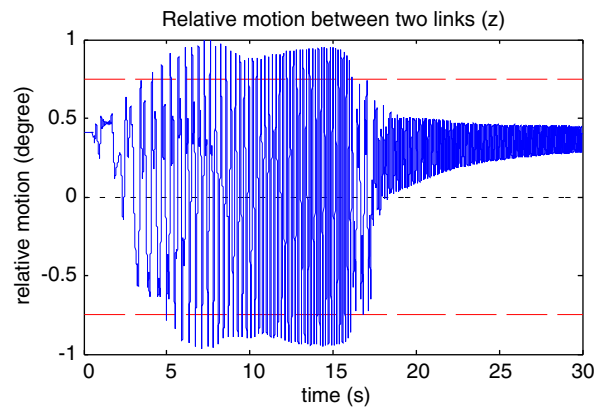


Fig. 8. Relative motion between both links (z): The solid line represents the relative motion measured by both encoders, while the dashed line shows the size of the backlash in the system.

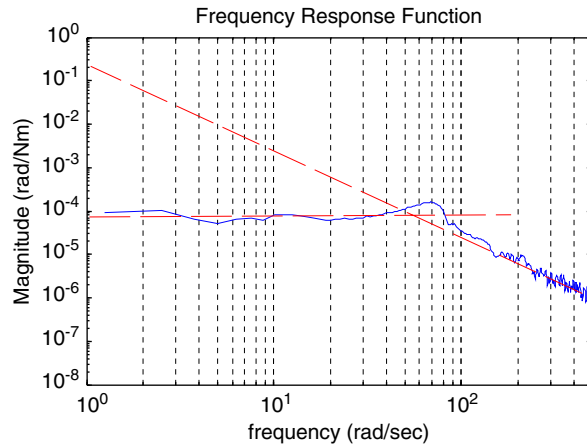


Fig. 9. Frequency response function of two-link mechanism: The link was preloaded onto one side using a low stiffness spring to eliminate non-linearity due to the backlash. The FRF obtained through shock excitation using impact hammer.

The two derivatives of $X(t)$ are then

$$\dot{X}(t) = X(t)[\dot{B}(t)/B(t) + j\omega_x(t)],$$

$$\ddot{X}(t) = X(t)[\ddot{B}(t)/B(t) - \omega_x^2(t) + 2j\dot{B}(t)\omega_x(t)/B(t) + j\dot{\omega}_x(t)]$$

Substituting all the analytic signals and their derivatives into Eq. (16) we get

$$Z \left\{ \left(\frac{\ddot{A}}{A} - \omega^2 + \omega_0^2 + 2h_0 \frac{\dot{A}}{A} \right) + j \left(2 \frac{\dot{A}}{A} \omega + \dot{\omega} + 2h_0 \omega \right) \right\} = -X \left\{ \left(\frac{\ddot{B}}{B} - \omega_x^2 \right) + j \left(2 \frac{\dot{B}}{B} \omega_x + \dot{\omega}_x \right) \right\} + CY. \quad (17)$$

Using the same procedures as for Eq. (3), i.e. by solving two equations for the real and imaginary parts of Eq. (17), we can obtain the expressions for instantaneous modal parameter as functions of first and second derivatives of signal envelopes and instantaneous frequencies of input and output displacement signal.

After identification, the restoring force, which illustrates the non-linear spring characteristic of the system, and the damping force can be obtained from the relations:

$$f_s(A) = A \omega_0^2(A), \quad (18)$$

$$f_d(\dot{A}) = 2h_0(A) \dot{A}. \quad (19)$$

5. Results and discussion

5.1. Envelope and instantaneous frequency

Envelope and instantaneous frequency calculations of the input and the output signals can be seen in Figs. 10 and 11, respectively. In the left panel of each figure, we can see the envelope estimation of displacement input and displacement output. The light dashed lines represent the envelope estimation based on HT technique without any filtration. The filtered HT curves represent the same technique after low-pass filtration of 0.5% of its half sampling rate (100% corresponds to half the sample rate), while WT curves represent that of Wavelet transform technique.

From those two figures, we can see that Wavelet analysis gives an improvement in envelope and instantaneous frequency extraction at several points. The most significant improvement is in the envelope and instantaneous frequency extraction of displacement output approximately after the first 17 s. If we refer to

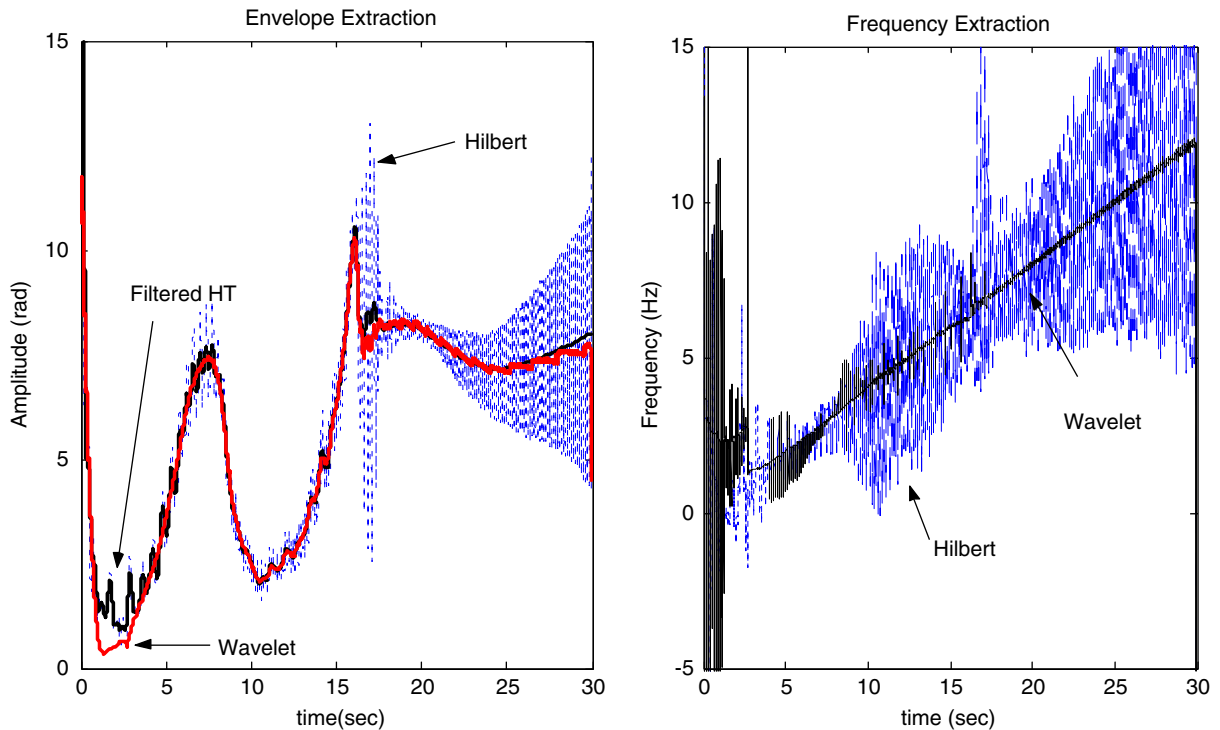


Fig. 10. Envelope and instantaneous frequency extraction of the input signal: Left figure shows the envelope extraction using both techniques. The dashed line represents the original Hilbert result; the dark-solid line represents the Hilbert result after 0.05% filtration, while the light-solid line corresponds to the extraction using Wavelet technique. The right figure shows the instantaneous frequency extraction results using both Hilbert (without any filtration) and Wavelet techniques.

Fig. 8, it is clearly seen that the response is shifted after 17 s. This might have happened because at the corresponding time, the level of displacement input has fallen below the backlash size in the system. As the envelope and the instantaneous frequency extraction using the Hilbert analysis for the signal with a certain offset cannot perform well, which means another superiority of Wavelet analysis.

At the time instant of 16–17 s, we can see a significant estimation error in instantaneous frequency. At this instant, the instantaneous frequency cannot be estimated, since the frequency content of the vibration response corresponds to the resonance frequency of the system (refer to Figs. 6 and 7).

5.2. Restoring force and damping force

The restoring force as function of displacement can be derived utilising Eq. (4). The plot of this restoring force is shown in Fig. 12. In the left panel of that figure, we can see the restoring force estimation based on HT technique with low-pass filtration of 1% of half of its sample rate, respectively. In the right side, we see the estimation based on Wavelet analysis. The size of backlash obtained from both techniques is close to the real backlash size introduced in the system. From the figures, by applying extrapolation on the reconstructed restoring force, we get the backlash size of 0.0258 rad ($= 1.48^\circ$ with standard deviation of error below 1.5%), where the real backlash size is approximately 1.5° from manual measurement. Let us note here, however, that since the identified part does not cover the whole range of the skeleton, we cannot ascertain the general validity of this result.

Referring to Eq. (4), the slope of the restoring force curve in Fig. 12 actually represents the modal stiffness of the system. After multiplying the slope by the moment of inertia of the second link, we can obtain the estimated stiffness value of the system. The modal stiffness parameter obtained by applying regression to the result is approximately 11 000 Nm/rad.

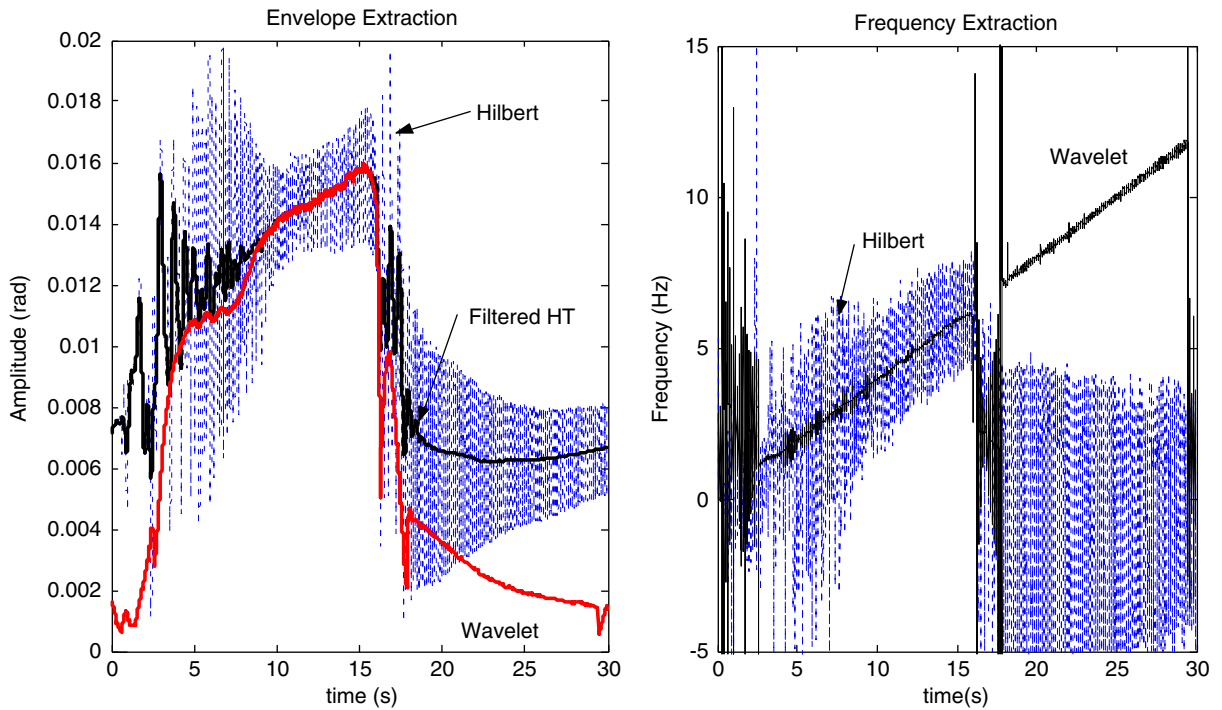


Fig. 11. Envelope and instantaneous frequency extraction of the output signal: Left figure shows the envelope extraction using both techniques. The dashed-line represents the original Hilbert result, while the dark-solid line corresponds to the Hilbert result after 0.05% filtration. The light-solid line represents the extraction using Wavelet technique. The right figure shows the instantaneous frequency extraction results using both Hilbert (without any filtration) and Wavelet techniques.

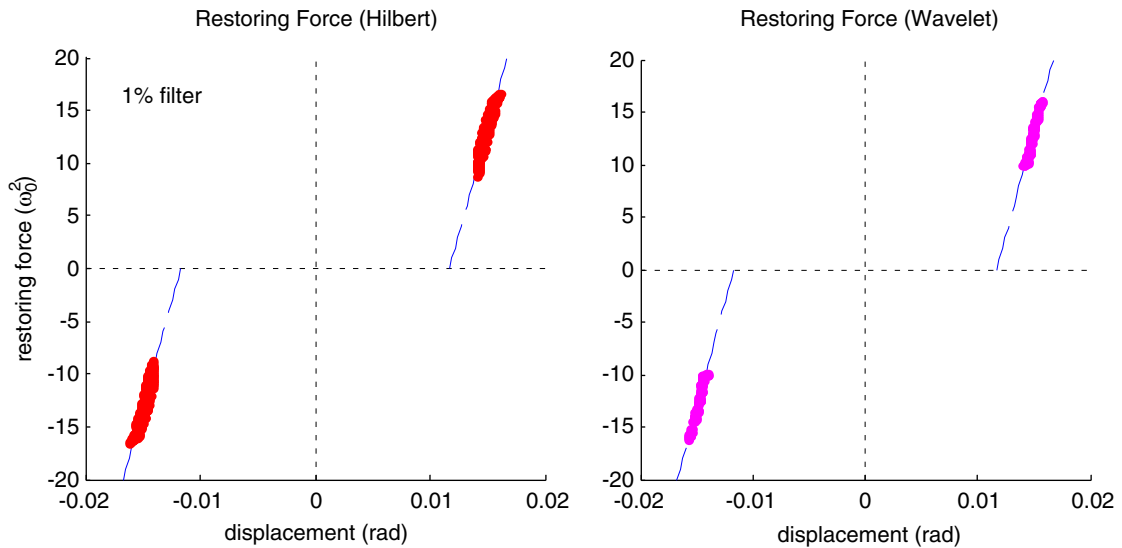


Fig. 12. Restoring force estimation based on Hilbert and Wavelet transform: The left figure shows the estimation of the restoring force based on the Hilbert analysis after 1% filtration, while the right figure depicts the result based on the Wavelet analysis.

The discontinuity appearing in the figures is due to the response at the resonance region as mentioned before. Hence, we cannot obtain the restoring force estimation in the corresponding region.

We can also identify the damping as a function of velocity by utilising Eq. (5). Fig. 13 shows the plot of the corresponding force, where the left figure shows the estimation based on the Hilbert analysis and the right one

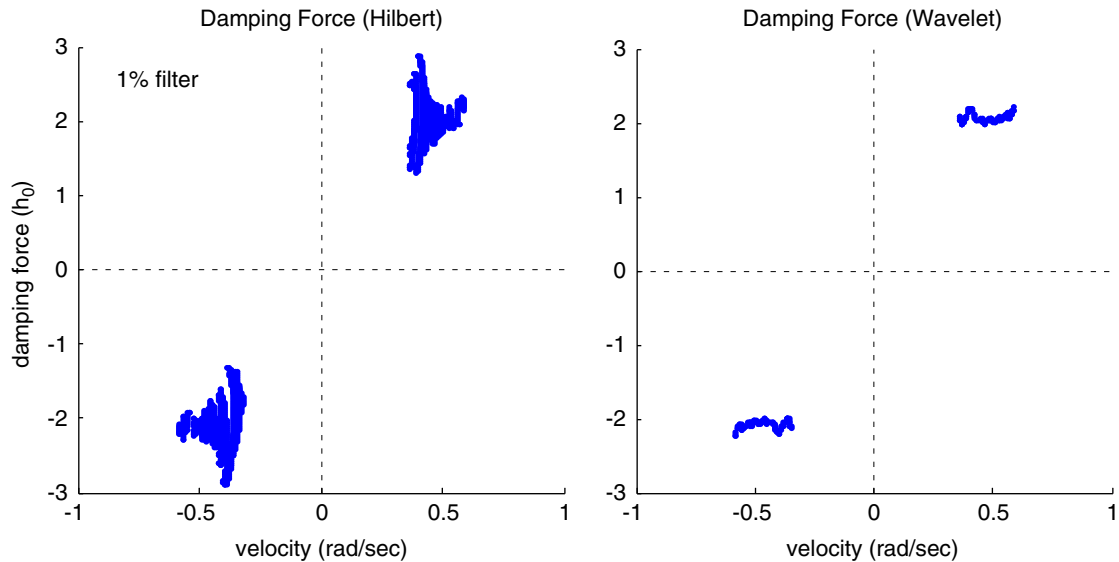


Fig. 13. Damping force estimation based on Hilbert and Wavelet transform: The left figure shows the estimation of the damping force based on the Hilbert analysis after 1% filtration, while the right figure depicts the result based on the Wavelet analysis.

demonstrates the result based on the Wavelet analysis. The Hilbert-based result shows imperfect reconstruction of the damping force and it suffers from more ripples than that of the restoring force. These are caused by the derivative form of the ‘noisy’ envelope function, \dot{A} , obtained from the Hilbert analysis, which is required in estimating the damping force as shown in Eq. (19).

Observing the behaviour, it is suspected that the damping force appears predominantly to be made up of friction, since a signum-like function, as we can see in the plot, leads us to the signature of the friction force.

6. Conclusion

Non-linear modal parameter estimation techniques based on Hilbert and Wavelet analyses are shown to be a good approximation of the true modal parameters characteristics. Both can estimate the backlash size satisfactorily; however, the Hilbert analysis needs low band filtration, which might lead to a misinterpretation of the result, and it is only applicable for the asymptotic signal. An improvement of the non-linear modal parameters estimation by introducing Wavelet analysis has been achieved owing to several advantages offered by the Wavelet properties. Wavelet analysis is capable of analysing envelope and instantaneous frequency of a shifted signal and the results have fewer ripples compared to those of HT. However, there are some drawbacks in the Wavelet-based technique. It needs not only a large amount of computation memory for its calculation process, since it deals with time–frequency domain, but also a long processing time.

A major difficulty in utilising the methods introduced in this paper concern the level of displacement input applied to the system. This displacement input should have an adequate level to ensure covering the backlash size. Due to the limitation of energy of excitation, this might become a problem, especially at high frequency. A limited level of excitation input will yield only a partial reconstruction of the restoring force characteristics.

Acknowledgement

The authors wish to acknowledge the partial financial support of this study by the Volkswagenstiftung under Grant no. I/76938.

References

- [1] Z.M. Elias, *Theory and Methods of Structural Analysis*, Wiley, New York, 1986.
- [2] F. Al-Bender, W. Symens, J. Swevers, H. Van Brussel, Theoretical analysis of the dynamic behavior of hysteresis elements in mechanical systems, *International Journal of Non-Linear Mechanics* 39 (2004) 1721–1735.
- [3] T. Prajogo, Experimental study of pre-rolling friction for motion-reversal error compensation on machine tool drive systems, Ph.D. Thesis, Department Werktuigkunde Katholieke Universiteit Leuven, 1999.
- [4] K. Worden, G.R. Tomlinson, *Nonlinearity in Structural Dynamics*, Institute of Physics Publishing, Bristol and Philadelphia, USA, 2001.
- [5] G.R. Tomlinson, Developments in the use of the Hilbert transform for detecting and quantifying nonlinearity associated with frequency response functions, *Mechanical System and Signal Processing* 1 (1987) 151–171.
- [6] M. Feldman, S. Braun, Analysis of typical nonlinear vibration systems by using the hilbert transform, In: *Proceeding of the XI International Modal Analysis Conference*, Kissimmee, Florida, 1993, pp. 799–805.
- [7] M. Feldman, Non-linear system vibration analysis using Hilbert transform-I. Free vibration analysis method ‘FreeVib’, *Mechanical Systems and Signal Processing* 8 (2) (1994) 119–127.
- [8] S. Braun, M. Feldman, Time–frequency characteristics of non-linear systems, *Mechanical Systems and Signal Processing* 11 (4) (1997) 611–620.
- [9] M. Feldman, Non-linear free vibration identification via the Hilbert transform, *Journal of Sound and Vibration* 208 (3) (1997) 475–489.
- [10] M. Feldman, S. Seibold, Damage diagnosis of rotors: application of Hilbert transform and multi-hypothesis testing, *Journal of Vibration and Control* 5 (1999) 421–445.
- [11] M. Feldman, Non-linear system vibration analysis using Hilbert transform-ii. forced vibration analysis method ‘ForceVib’, *Mechanical Systems and Signal Processing* 8 (3) (1994) 309–318.
- [12] M. Ruzzene, L. Fasana, L. Garibaldi, B. Piombo, Natural Frequencies and dampings identification using wavelet transform: application to real data, *Mechanical Systems and Signal Processing* 11 (2) (1997) 207–218.
- [13] W.J. Staszewski, Identification of nonlinear systems using multi-scale ridges and skeletons of the wavelet transform, *Journal of Sound and Vibration* 214 (4) (1998) 639–658.
- [14] W.J. Staszewski, J.E. Chance, J.E. Identification of nonlinear systems using wavelets—experimental study, In: *Proceedings of the XV International Modal Analysis Conference*, Orlando, FL, 1997, pp. 1012–1016.
- [15] T. Tjahjowidodo, F. Al-Bender, H. Van Brussel, Quantifying chaotic responses of mechanical systems with backlash component, *Mechanical Systems and Signal Processing* (2005), accepted, doi:10.1016/j.mssp.2005.11.003.
- [16] M. Misiti, Y. Misiti, G. Oppenheim, J.M. Poggi, *Wavelet Toolbox for Use with Matlab*, The MathWorks, July 2002 (online only).